

Menin-MLL inhibitors induce ferroptosis and enhance the anti-proliferative activity of auranofin in several types of cancer cells

ICHIROH KATO^{1,2}, TAKASHI KASUKABE¹ and SHUNICHI KUMAKURA¹

¹Department of Medical Education and Research, Faculty of Medicine, Shimane University, Izumo, Shimane 693-8501;

²Oki Hospital, Okinoshima-cho, Shimane 685-0016, Japan

Received May 26, 2020; Accepted August 13, 2020

DOI: 10.3892/ijo.2020.5116

Abstract. Menin-mixed-lineage leukemia (MLL) inhibitors have potential for use as therapeutic agents for MLL-rearranged leukemia. They are also effective against solid cancers, such as breast cancer. The present study demonstrated that menin-MLL inhibitors, such as MI-463, unexpectedly induced the ferroptotic cell death of several cancer cell lines. MI-463 at a double-digit nM concentration markedly decreased the viable number of OVCAR-8 ovarian cancer cells for 3 days. Ferrostatin-1 (a ferroptosis inhibitor) almost completely abrogated the MI-463-induced decrease in viable cell numbers. Furthermore, the cancer cell-killing activity was inhibited by *N*-acetylcysteine [a scavenger of reactive oxygen species (ROS)], deferoxamine (DFO, an iron chelator), PD146176 (a specific inhibitor of arachidonate 15-lipoxygenase), idebenone (a membrane-permeable analog of CoQ₁₀) and oleic acid [a monounsaturated fatty acid and one of the end products of stearoyl-CoA desaturase 1 (SCD1)], whereas Z-VAD-FMK (an apoptosis inhibitor) had a negligible effect on cell death. It was also found that MI-463 in combination with auranofin (a thioredoxin reductase inhibitor) synergistically increased cancer the death of breast, ovarian, pancreatic and lung cancer cell lines (88%, 14/16 cell lines). The synergistic induction of cell death was abrogated by ferroptosis inhibitor and DFO. Inhibitors of SCD1, similar to MI-463, also enhanced cancer cell death synergistically with auranofin, while inhibitors of SCD1 and MI-463 did not additively induce cell death. Treatment with zinc protoporphyrin-9, a specific inhibitor of heme oxygenase-1 (HO-1), markedly attenuated the cell death induced by MI-463 plus auranofin. On the whole, these results

suggest that the MI-463-induced decrease in cell viability may be at least partly associated with the inhibition of SCD1 activity. In addition, the potent induction of HO-1 contributed to the synergistic effects of MI-463 plus auranofin. Therefore, menin-MLL inhibitors, such as MI-463, in combination with auranofin represent an effective therapeutic approach for several types of cancer via the induction of ferroptosis.

Introduction

Chromatin regulators have emerged as promising targets of small-molecule compounds in several types of human cancer (1,2). Menin is a scaffold protein of the mixed-lineage leukemia (MLL)/complex proteins associated with Set1 (COMPASS)-like complex, directly interacting with MLL (histone methyltransferase), and is critical for MLL activity and the maintenance of MLL-rearranged leukemia (3-5). The inhibition of the menin-MLL interaction with small-molecule inhibitors, such as MI-463, MI-503, MI-3454 and VTP50469, has been shown to inhibit the proliferation and induce the differentiation of MLL1-rearranged and nucleophosmin 1 (NPM1)-mutated leukemia (3-5). In addition to leukemia, previous studies have demonstrated that the interaction between menin and MLL also plays an important role in the maintenance and growth of solid tumors, such as breast cancer, pancreatic cancer, prostate cancer, Ewing sarcoma and hepatocellular carcinoma (HCC) (2,6-9). In breast cancer, p53 gain-of-function (GOF) mutants bind to and upregulate chromatin regulatory genes, such as MLL1, resulting in genome-wide increases in histone methylation. The genetic knockdown of MLL has been shown to reduce the proliferation of BT-549 (mutant p53 249S) and MDA-MB-468 (mutant p53 R273H) cells, but does not markedly affect the proliferation of MCF-7 (wild-type p53) cells (2). Dreijerink *et al* (6) reported that menin-MLL plays an oncogenic role in estrogen receptor (ER)⁺ MCF-7 breast cancer cells. The menin-MLL complex is associated with active gene promoters in ER⁺ breast cancer cells. It is also present at FOXA1 and GATA3-bound enhancers, which associate with promoters through chromatin looping (6). Therefore, menin co-regulates the proliferative breast cancer-specific gene expression program in ER⁺ breast cancer cells, although

Correspondence to: Professor Takashi Kasukabe, Department of Medical Education and Research, Faculty of Medicine, Shimane University, 89-1 Enya-cho, Izumo, Shimane 693-8501, Japan
E-mail: kasukabe@med.shimane-u.ac.jp

Key words: menin-MLL inhibitor, MI-463, MI-503, MI-2-2, auranofin, ferroptosis, ovarian cancer cells, breast cancer cells, pancreatic cancer cells

menin regulates anti-proliferative genes in normal mammary progenitor cells (6). In prostate cancer, the MLL complex functions as a co-activator of androgen receptor (AR) signaling. AR directly interacts with the MLL complex via the menin-MLL subunit. A high menin expression is associated with the poor overall survival of patients diagnosed with prostate cancer. The inhibition of the menin-MLL interaction with a small-molecule inhibitor has been shown to impair AR signaling and suppress the growth of castration-resistant tumors *in vivo* in mice (7). MLL1 and menin expression levels are high in Ewing sarcoma. The continued expression of both proteins is required for the maintenance of tumorigenicity. The inhibition of the menin-MLL interaction with a small-molecule inhibitor, such as MI-503, has been shown to result in the loss of tumorigenicity (8). The protein-protein interaction between menin and MLL1 has been shown to play an important role in the development of HCC. MI-503 also exhibits antitumor activity in *in vitro* and *in vivo* models of HCC (9). These findings suggest the potential of the menin-MLL interaction as a therapeutic target in several types of cancer, as well as in leukemia, and also that small-molecule inhibitors of the menin-MLL interaction may suppress the proliferation of cancer cells without MLL-fusion genes. However, limited information is currently available on the mechanisms contributing to the induction of cell death by small-molecule inhibitors of the menin-MLL interaction.

Ferroptosis, a recently discovered form of regulated cell death, is dependent on the presence of intracellular iron and the accumulation of reactive oxygen species (ROS) (10). Due to the enhanced dependence of cancer cells on iron, the induction of ferroptosis is becoming a promising therapeutic strategy. In contrast to apoptosis, which numerous cancer cells can evade, ferroptosis is lethal to numerous tumor cells that have become dependent on the suppression of ferroptosis for their survival, including some of the most drug-resistant and aggressive cancer cells, including persister cells and cells that have undergone epithelial-mesenchymal transition (10,11). Thus, the induction of ferroptosis may provide novel therapeutic avenues for the treatment of drug-resistant cancers (11,12). Ferroptotic death is modulated by the pharmacological perturbation of lipid repair systems involving glutathione (GSH) and glutathione peroxidase 4 (GPX4), and is dependent on a set of positive-acting enzymatic reactions, including the biosynthesis of polyunsaturated fatty acid (PUFA)-containing phospholipids and the selective oxygenation of PUFA-phosphatidylethanolamines by lipoxygenases (13). Recent studies (14,15) have demonstrated that the coenzyme Q₁₀ (CoQ₁₀) oxidoreductase ferroptosis suppressor protein 1 (FSP1) functions in parallel with GPX4 and GSH to inhibit ferroptosis, and also that myristoylation recruits FSP1 to the plasma membrane, where it functions as an oxidoreductase that reduces CoQ₁₀, which acts as a lipophilic radical-trapping antioxidant that prevents the propagation of lipid peroxides. Tesfay *et al* (16) recently demonstrated that stearoyl-CoA desaturase 1 (SCD1) was expressed at high levels in different isotypes of ovarian cancer and that it protected ovarian cancer cells from ferroptotic cell death. Furthermore, the pharmaceutical inhibition of SCD1 induced ferroptosis and apoptosis *in vitro* and *in vivo*. These findings suggest that the use of a combined treatment with inhibitors of these ferroptosis suppressors and ferroptosis inducers has potential

as a novel therapeutic strategy for patients with various types of cancer, including ovarian cancer.

In the present study, it was demonstrated that menin-MLL inhibitors, such as MI-463, MI-503 or MI-2-2, unexpectedly induced the ferroptotic death, but not the apoptotic death of several cancer cell line cells, including ovarian cancer and breast cancer cell lines. Furthermore, the results obtained revealed that MI-463 in combination with auranofin [a thio-redoxin reductase (TrxR) inhibitor] induced a synergistic increase in the death of breast, ovarian, pancreatic and lung cancer cell lines. The synergistic induction of cell death was also abrogated by ferroptosis inhibitors, such as ferrostatin-1 (Ferr-1) and deferoxamine (DFO).

Materials and methods

Materials and reagents. MI-463 was purchased from ChemScene. MI-503 and VTP50469 was obtained from MedChem Express. RPMI-1640, 3-(4,5-dimethylthiazol-2-yl)-2,5-diphenyltetrazolium bromide (MTT), *N*-acetylcysteine (NAC), Ferr-1, DFO, ciclopirox (CPX), OICR-9429, MF-438, echinomycin, protoporphyrin IV cobalt chloride (CoPP) and MI-2-2 were purchased from Sigma-Aldrich; Merck KGaA. Z-VAD, Nec-1s, Liprox and Piribedil were purchased from Selleckchem. PD146176, CAY10566, idebenone and zinc protoporphyrin-IV (ZnPP) were obtained from Cayman Chemical Co. Oleic acid was purchased from FUJIFILM Wako Pure Chemical Corporation. Auranofin was obtained from AdipoGen Life Sciences. 5-Fluorouracil, actinomycin D, cisplatin, gemcitabine, paclitaxel, docetaxel, bortezomib, romidepsin and suberoylanilide hydroxamic acid (SAHA) were purchased from Sigma-Aldrich; Merck KGaA. Tin protoporphyrin IV was purchased from R&D Systems, Inc. Anti-cleaved poly(ADP-ribose) polymerase (PARP; cat. no. 5625), anti-cleaved caspase-3 (cat. no. 9664) and anti- β -tubulin (cat. no. 86298) antibodies were purchased from Cell Signaling Technology, Inc.

Cells and cell culture. Human ovarian cancer cell lines (OVCAR-8, OVCAR-3 and OVCAR-4) and lung carcinoma cell lines (A549, LU99, LU65 and PC-7) were gifts from Dr Honma (Shimane University, Shimane, Japan) (17,18). Two breast carcinoma cell lines (BT-549 and MDA-MB-468) were gifts from Dr Takenaga (Shimane University, Shimane, Japan) and Dr Yamaguchi (Saitama Cancer center, Saitama, Japan), respectively. The other breast carcinoma cell lines (MDA-MB-231, MCF-7 and T47D) were used from laboratory stock previously reported by the authors (19). Pancreatic carcinoma cell lines (MIA PaCa-2, PANC-1, BxPC-3 and CFPAC-1) were purchased from ATCC. All cancer cell line cells were cultured in RPMI-1640 medium supplemented with 10% fetal bovine serum and 80 μ g/ml gentamicin at 37°C in a humidified atmosphere of 5% CO₂ in air.

Assay of growth inhibitory activities of various anticancer agents in BT-549 cells with MI-463. BT-549 cells seeded at 1.5x10⁴ cells/ml in a 24-well multi-dish. The cells were cultured with auranofin (10-1,000 nM), 5-fluorouracil (2-20 μ M), actinomycin D (0.1-1.5 nM), cisplatin (100-1,000 nM), gemcitabine (1-40 nM), paclitaxel (1-5 nM), docetaxel

(0.1-1 nM), romidepsin (0.1-1 nM), or SAHA (100-2,000 nM) in the presence or absence of 0.16 μ M MI-463 for 5 days. The number of viable cells was then measured by MTT assay as previously described (20). The growth-inhibitory activities of the anticancer agents with or without MI-463 were examined by determining the concentrations of inhibitors required to reduce the cell number to one-half of that in untreated cells (IC_{50}). The levels of potentiation of growth inhibitory activities of anticancer agents by MI-463 were shown as the ratios of the IC_{50} without MI-463 to the IC_{50} with MI-463.

Assay of cell growth and viability. Cell numbers were counted in a Model Z1 Coulter Counter (Beckman Coulter, Inc.). The cells were seeded at $1-2 \times 10^4$ cells/ml in a 24-well multi-dish. Following culture with or without the test compounds for the indicated periods of time, viable cells were examined using a modified MTT assay, as previously described (20) or trypan blue dye exclusion test using the automated cell counter model R1 (Olympus Corporation).

Assay of long-term cell numbers. Cells (1.5×10^4 /ml) were cultured in medium with the test compounds. Thereafter, the cell density of the treated cells was kept at $2-50 \times 10^4$ /ml to maintain the growth phase. The medium of treated cultures was replaced with fresh medium with or without the test compounds every 5 days. The cumulative cell number was calculated from viable cell counts and the dilution used when feeding the culture. Viable cell numbers were counted using the trypan blue dye exclusion test with the automated cell counter model R1 (Olympus Corporation).

Measurement of ROS generation. The production of ROS was monitored using a Muse cell analyzer (EMD Millipore), and the experimental protocol followed the description provided with the kit (Muse Oxidative Stress kit, EMD Millipore), as previously described (21). OVCAR-8 cells were treated with 0.16 or 0.31 μ M MI-463 for 8 and 24 h to induce ROS production, and ROS levels were then measured using the Muse Oxidative Stress kit. Two populations of cells were distinguished in this assay: ROS (-) (live cells) and ROS (+) (cells producing ROS).

Measurement of the cell cycle. Cell cycle analysis was measured using a Muse cell analyzer (EMD Millipore), and the experimental protocol followed by the description provided with the kit (Muse Cell Cycle kit, EMD Millipore). OVCAR-8 cells were treated with or without 0.2 or 0.5 μ M DFO for 3 days. Following the treatment period, cells were collected, washed and fixed overnight in 70% ethanol in PBS at -20°C . Fixed cells were pelleted and stained with cell cycle analysis reagent for 30 min at 37°C in the dark according to the manufacturer instructions, and approximately 5,000 events were analyzed on a Muse cell analyzer (EMD Millipore).

Malondialdehyde (MDA) assay. The relative MDA concentration in cell lysates was assessed using a Lipid Peroxidation Assay kit (#ab118970, Abcam) according to the manufacturer's instructions. Briefly, the MDA in the sample reacted with thiobarbituric acid to generate a MDA-thiobarbituric acid adduct. The MDA-thiobarbituric acid adduct was quantified

colorimetrically (optical density, 532 nm) using a microplate reader (GloMax Discover GM3000; Promega Corp.).

Western blot analysis. Cells were packed after washing with cold PBS and then lysed at a concentration of 1×10^7 cells/ml in lysis buffer CellLytic™-M (Sigma-Aldrich; Merck KGaA) supplemented with a proteinase inhibitor cocktail and phosphatase inhibitor cocktail 2/3 (Sigma-Aldrich; Merck KGaA). Equal amounts of protein were separated on 10-20% SDS-polyacrylamide gels (FUJIFILM Wako Pure Chemical Corporation). Proteins were electrophoresed on gels and transferred onto Immobilon-P membranes (EMD Millipore) using the primary antibodies (1:1,000 dilution) at 4°C overnight. An anti-rabbit (cat. no. 7074) or anti-mouse (cat. no. 7076) IgG HRP-linked antibody (Cell Signaling Technology, Inc.) was used as a secondary antibody (1:2,000 dilution) at room temperature for 60 min. Bands were identified by a treatment with Clarity ECL Substrate (Bio-Rad Laboratories, Inc.) at room temperature for 5 min and detected using a Fuji Lumino Image Analyzer LAS-4000 system (Fuji Film Co., Ltd.), as previously described (21). For the quantification of the blots, densitometry was performed using MaltiGauge ver 3.0 software (Fuji Film Co., Ltd.). All western blots shown are representative of at least 3 independent experiments.

RNA extraction and measurement of mRNA levels by reverse transcriptase (RT)-quantitative polymerase chain reaction (qPCR). RNA was extracted using an RNeasy Plus Mini kit (Qiagen, Inc.) according to the manufacturer's instructions. Total RNA (1 μ g) from the cancer cells was reverse transcribed using the ReverTra Ace qPCR RT kit (Toyobo Co., Ltd.). qPCR using the SYBER-Green method was performed with Thunderbird SYBER qPCR Mix (Toyobo Co.) on a Thermal Cycler Dice Real-time PCR instrument (Takara Bio, Inc.) according to the manufacturer's instructions and as previously described (22). The heme oxygenase-1 (HO-1) primers used for qPCR were as follows: Forward, 5'-CAGGCAGAGAAT GCTGAGTTC-3' and reverse, 5'-GCTTCACATAGCGCT GCA-3' (23). The GAPDH primers used for qPCR were as follows: Forward, 5'-GACGCTGGGGCTGGCATTG-3' and reverse, 5'-GCTGGTGGTCCAGGGGGTC-3' (22). The amplification efficiencies of HO-1 and GAPDH were 0.980 and 0.984, respectively.

Statistical analysis. Values were compared using the two-tailed Student's t-test. Differences among multiple groups was analyzed by one-way ANOVA followed by Tukey's post hoc test, using GraphPad Prism 8 software. $P < 0.05$ was considered to indicate a statistically significant difference.

Results

Menin-MLL inhibitors induce ferroptotic cancer cell death. The OVCAR-8 human ovarian cancer cells were pre-treated with 1 μ M Ferr-1 (ferroptosis inhibitor and lipid peroxidation inhibitor) for 2 h and were then further cultured in the presence or absence of MI-463 (Fig. 1A), MI-503 (Fig. 1B) and MI-2-2 (Fig. 1C) for 3 days. The number of viable cells was determined by MTT assay following 3 days of exposure to various concentrations of MI-463, MI-503, or MI-2-2. The

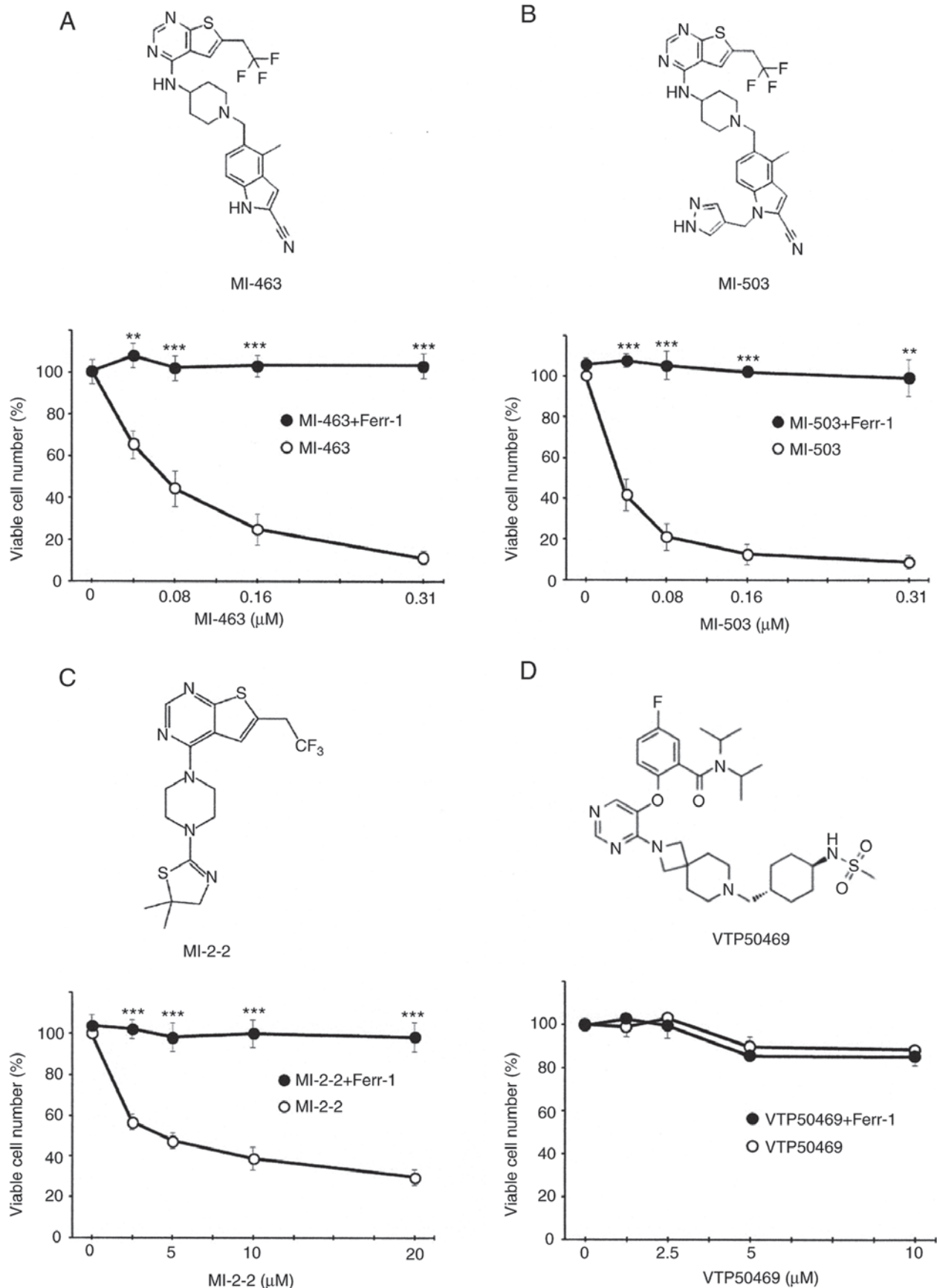


Figure 1. Effects of ferrostatin-1 (Ferr-1) on the menin-MLL inhibitor-induced cell death of OVCAR-8 cells. Structures of (A) MI-463 (upper panel), (B) MI-503 (upper panel), (C) MI-2-2 (upper panel) and (D) VTP50469 (upper panel). OVCAR-8 cells (1.5×10^4 cells/ml) were cultured with the indicated concentrations of (A) MI-463 (bottom panel), (B) MI-503 (bottom panel), (C) MI-2-2 (bottom panel) and (D) VTP50469 (bottom panel) in the absence (open circles) or presence of $1 \mu\text{M}$ ferrostatin-1 (Ferr-1) (closed circles) for 3 days. Cells were treated with Ferr-1 for 2 h prior to the MI-463, MI-503, MI-2-2, or VTP50469 treatment. Data are representative of the means \pm SD of 3 measurements. ** $P < 0.01$ and *** $P < 0.001$ vs. (A) MI-463, (B) MI-503 and (C) MI-2-2 at the indicated concentrations.

IC₅₀ values were calculated by determining the concentrations of these inhibitors required to reduce the cell number to half that of the untreated cells. These menin-MLL inhibitors dose-dependently decreased the OVCAR-8 viable cell numbers: The IC₅₀ (concentration of the drug required for 50% inhibition of cell growth) values of MI-463, MI-503 and MI-2-2 were 0.06, 0.04 and 4.5 μ M, respectively (Fig. 1A-C, bottom panels). Ferr-1 almost completely abrogated the MI-463-, MI-503- and MI-2-2-induced decrease in the viable number of OVCAR-8 cells (Fig. 1A-C, bottom panels). These results suggested that these menin-MLL inhibitors induced ferroptotic cancer cell death and that both MI-463 and MI-503 were potent ferroptosis inducers of OVCAR-8 cell death. However, VTP50469 could not induce the death of OVCAR-8 cells even at a high concentration (10 μ M) (Fig. 1D).

Since ferroptosis is a recognized ROS- and iron-dependent form of regulated cell death that is accompanied by the accumulation of lipid peroxidation, the effects of NAC (a ROS scavenger) on the MI-463-induced decrease in viable cell numbers were examined (Fig. 2A). NAC (2 mM) evidently abolished MI-463-induced cell death. The generation of ROS was also measured using the Muse cell analyzer. OVCAR-8 cells were treated with 0.16 or 0.31 μ M MI-463 for 8 or 24 h and ROS levels were then examined using the Muse Oxidative Stress kit. Treatment with MI-463 (0.16 μ M) induced an approximately 2-fold increase in the ROS high cell population at 8 h and an approximately 5-fold increase in the ROS high cell population at 24 h (Fig. 2B). The typical iron chelator DFO (1 μ M) potently inhibited MI-463-induced cancer cell death (Fig. 2C). Although treatment with 0.25 or 0.5 μ M DFO did not affect the cell cycle or proliferation of OVCAR-8 cells, 0.25 or 0.5 μ M DFO was able to attenuate the MI-463-induced death of OVCAR-8 cells (data not shown). These results suggest that the attenuation of ferroptotic cell death by iron chelators is not involved in the alteration of the cell cycle status. CPX (another intracellular iron chelator) also significantly suppressed MI-463-induced cell death (Fig. 2D). On the other hand, Z-VAD (a typical apoptosis inhibitor) failed to protect the cells against MI-463-induced cell death (Fig. 2E). Consistent with the established role of lipoxygenase-catalyzed lipid hydroperoxidation in ferroptosis, it was found that treatment with the specific inhibitor of arachidonate 15-lipoxygenase, PD146176, protected the cancer cells against MI-463-induced cell death (Fig. 2F). Furthermore, idebenone (a lipophilic antioxidant and soluble analog of CoQ₁₀) markedly inhibited MI-463-induced cancer cell death (Fig. 2G). A recent study (16) demonstrated that SCD1 protected ovarian cancer cells from ferroptotic cell death and that oleic acid (one of the end products of SCD1) protected against inhibitors of SCD1-induced cell death and RSL3-induced ferroptotic cell death (a typical ferroptosis inducer). In the present study, oleic acid almost completely protected the cancer cells against MI-463-induced death (Fig. 2H). Collectively, these results suggest that MI-463 induces cancer cell death through the induction of ferroptosis in OVCAR-8 cells.

MI-463 enhances the anti-proliferative activity of auranofin in several types of cancer cells. The present study then investigated whether MI-463 induces the ferroptotic death of other types of cancer cells. MI-463 also dose-dependently suppressed the viable number of BT-549 triple-negative

breast cancer cells (Fig. 3A). The BT-549 cells (IC₅₀ value, 0.40 μ M) were less sensitive to MI-463 than the OVCAR-8 cells (IC₅₀ value, 0.06 μ M) (Fig. 1A). Ferr-1 almost completely reversed the MI-463-induced death of BT-549 cells (Fig. 3A). These results suggest that menin-MLL inhibitors, such as MI-463, induce the ferroptosis not only of OVCAR-8 cells, but also of other types of cancer cells.

Subsequently, the present study examined whether the new ferroptosis inducer, MI-463, potentiates the growth inhibitory activity of various anticancer agents using BT-549 triple-negative breast cancer cells. To assess the effects of anticancer agents and MI-463 on the growth of BT-549 cells, the number of viable cells was measured by MTT assay following a 5-day exposure to various concentrations of anticancer agents with or without 0.16 μ M MI-463. The growth inhibitory activities of the drugs were examined by measuring the IC₅₀ values. Sensitivity to the majority of anticancer agents, apart from gemcitabine and paclitaxel, was significantly enhanced by MI-463. It was found that the anti-proliferative activity of auranofin was enhanced most potently (>6-fold) by MI-463 (Table I). As shown in Fig. 3B, MI-463 (0.31 μ M) significantly enhanced the auranofin-induced suppression of viable cell numbers. Although auranofin alone at 0.2 μ M decreased the viable number of BT-549 cells to ~70% of the control (Fig. 3B) and MI-463 (0.31 μ M) alone to approximately 59-65% of the control (Fig. 3A and B), combined treatment with BT-549 and auranofin decreased the viable number of BT-549 cells to ~5% of the control (Fig. 3B).

Zhu *et al* previously reported that the genetic knockdown of MLL decreased the proliferation of BT-549 (mutant p53 249S) cells, but had a negligible effect on the proliferation of MCF-7 (wild-type p53) cells (2). The inhibition of the functions of MLL1 was also demonstrated by targeting its interaction with the WDR5 subunit of the MLL/COMPASS complex (2). OICR-9429, an antagonist of the interaction of WDR5 with MLL1, also exerted a dose-dependent inhibitory effect on GOF p53 cell growth (2). The present study then investigated whether OICR-9429 and auranofin also synergistically reduce viable cell numbers. In contrast to MI-463, OICR-9429 and auranofin only exerted additive effects on the suppression of viable BT-459 cells (Fig. 3C). Another MLL/WDR5 protein-protein interaction inhibitor (Piribedil) (23) and auranofin also did not exert synergistic effects on the suppression of viable BT-459 cells (data not shown). These results suggested that the synergistic effects of MI-463 and auranofin were not involved in the inhibitory effects of MLL/WDR5 protein-protein interaction inhibitors. The time course of the combined effects of MI-463 and auranofin on the viable number of BT-549 cells is presented in Fig. 3D. The viable number of BT-549 cells was moderately reduced by MI-463 (0.31 μ M) or auranofin (0.2 μ M) alone, and the proliferation of viable cells was still observed at 4 days; however, the viable cell number did not change until 2 days following combined treatment and then slightly decreased (Fig. 3D). The time course of the combined effects of MI-463 and auranofin on the viability of BT-549 cells examined by the trypan blue dye exclusion test is presented in Fig. 3E. The viability of the BT-549 cells was maintained at a level >80% in the presence of MI-463 or auranofin alone, whereas combined treatment with MI-463 and auranofin decreased viability to ~60% at 2 days and to almost 0% following 3 days of treatment (Fig. 3D). The long-term effects of combined treatment

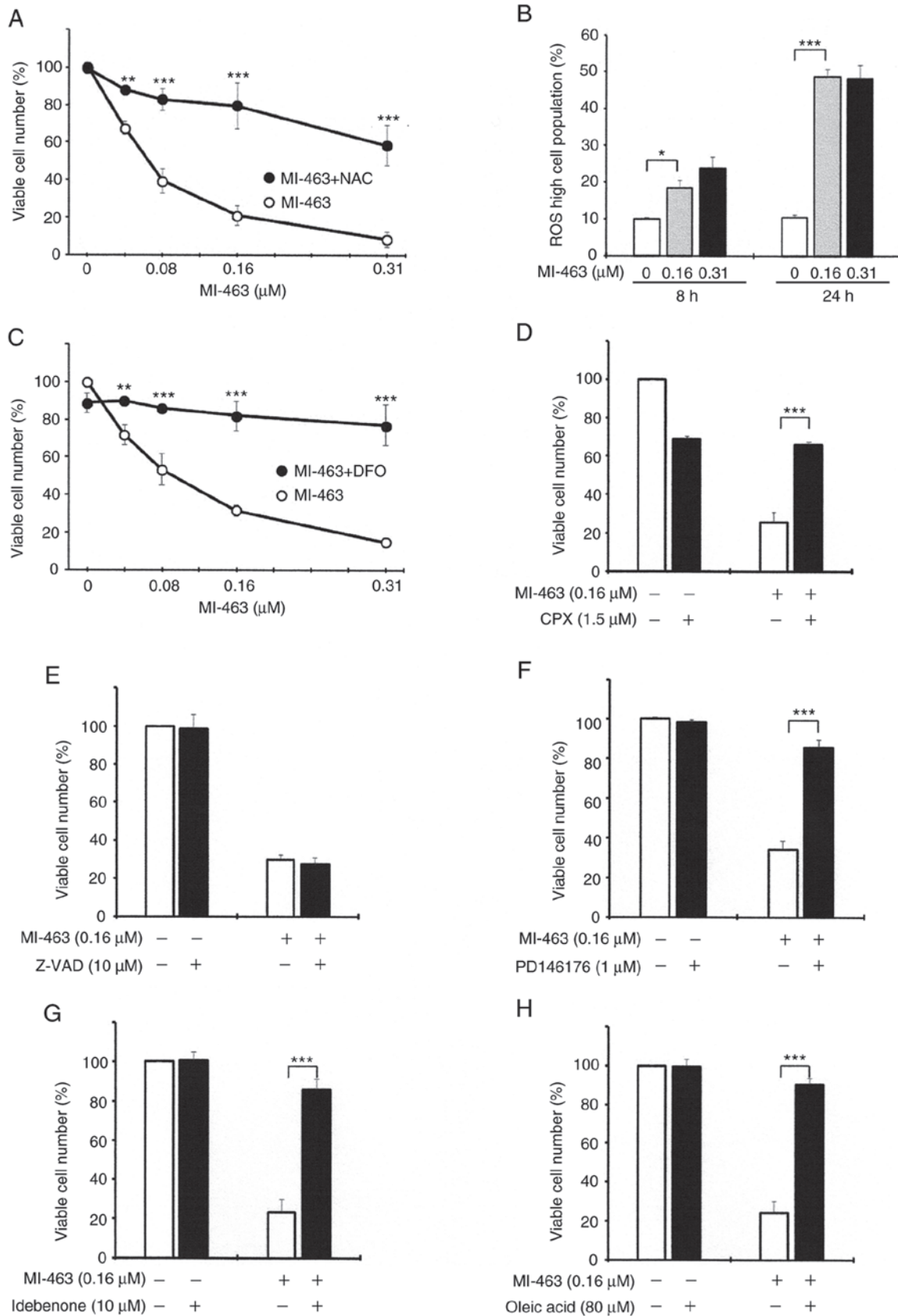


Figure 2. Effects of several ferroptosis inhibitors on the MI-463-induced of OVCAR-8 cells. OVCAR-8 cells (1.5×10^4 cells/ml) were cultured with the indicated concentrations of MI-463 in the absence (open circles) or presence of 2 mM (A) N-acetylcysteine (NAC) or (C) deferoxamine (DFO) (closed circles) for 3 days. Cells were treated with NAC or DFO for 2 h prior to the MI-463 treatment. Data are representative of the means \pm SD of 3 measurements. ** $P < 0.01$ and *** $P < 0.001$ vs. MI-463 at the indicated concentrations. (B) OVCAR-8 cells were cultured with 0.16 μM (gray columns) or 0.31 μM (closed columns) MI-463 for 8 or 24 h and ROS levels were then measured using the Muse Oxidative Stress kit. OVCAR-8 cells were cultured with 0.16 μM MI-463 in the absence (open columns) or presence (closed columns) of (D) 1.5 μM ciclopirox (CPX), (E) 10 μM Z-VAD-FMK (Z-VAD), (F) 1 μM PD146176, (G) 10 μM idebenone, or (H) 80 μM oleic acid for 3 days. Cells were treated with CPX, Z-VAD, PD146176, idebenone, or oleic acid for 2 h prior to the MI-463 treatment. Viable cell numbers were then measured by MTT assay. Data are representative of the means \pm SD of 3 measurements. * $P < 0.05$ and *** $P < 0.001$.

Table I. Potentiation of growth inhibitory activities of various anticancer agents in BT-549 cells treated with MI-463.

Anticancer agent (nM)	Growth inhibition (IC ₅₀)		Ratio (-/+) ^a
	- MI-463	+ MI-463	
Auranofin	353±51	55±18	6.41
5-Fluorouracil	1,7500±2,800	4,500±350	3.89
Actinomycin D	1.35±0.34	0.33±0.08	4.09
Cisplatin	340±38	130±35	2.61
Gemcitabine	10±0.9	7.5±0.6	1.33
Paclitaxel	3.5±0.21	2.2±0.32	1.59
Docetaxel	0.9±0.15	0.4±0.07	2.25
Bortezomib	20±4.6	8.4±1.1	2.38
Romidepsin	0.64±0.08	0.15±0.06	4.27
SAHA	1,316±280	250±39	5.26

^aRatio (-/+), IC₅₀ without MI-463: IC₅₀ with MI-463. Values are the means ± SD of 3 measurements. SAHA, suberoylanilide hydroxamic acid.

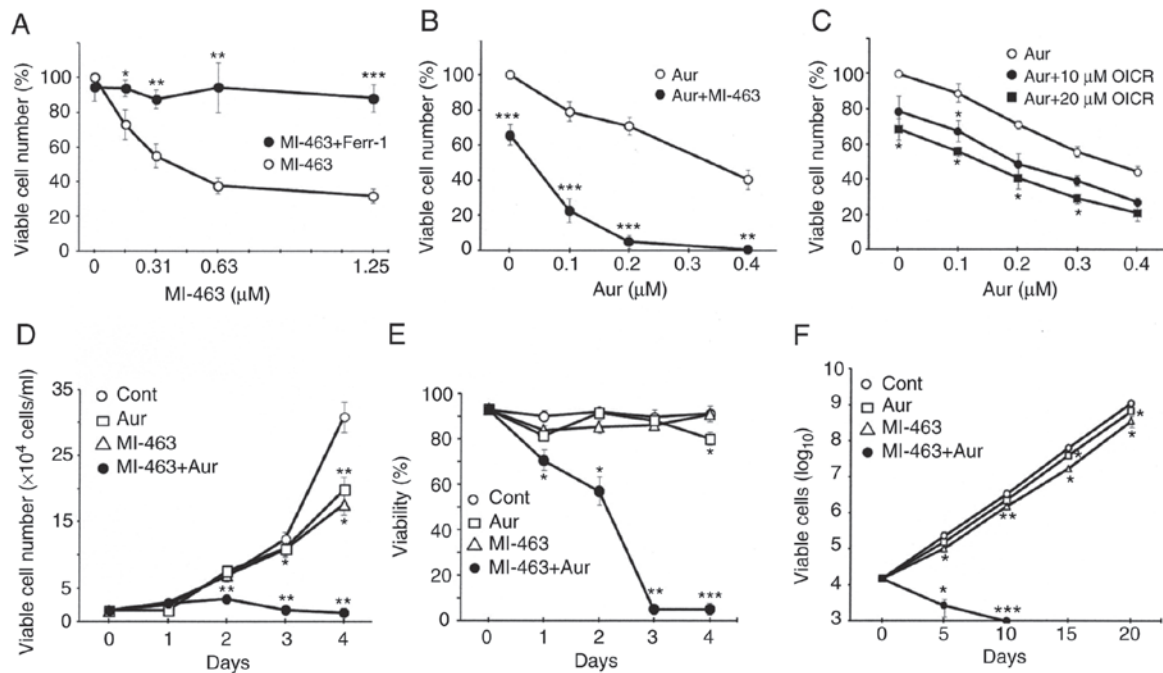


Figure 3. Effects of combined treatment with MI-463 and auranofin (Aur) on the viability of BT-549 cells. (A) BT-549 cells (1.5×10^4 cells/ml) were cultured with the indicated concentrations of MI-463 in the absence (open circles) or presence of $1 \mu\text{M}$ Ferr-1 (closed circle) for 3 days. Cells were treated with Ferr-1 for 2 h prior to MI-463 treatment. * $P < 0.05$, ** $P < 0.01$ and *** $P < 0.001$ vs. MI-463 at the indicated concentrations. (B and C) BT-549 cells were cultured with the indicated concentrations of auranofin (Aur) in the absence (open circles) or presence of (B) $0.31 \mu\text{M}$ MI-463 (closed circle) or (C) $10 \mu\text{M}$ (closed circles) or $20 \mu\text{M}$ (closed squares) OICR-9429 (OICR) for 4 days. Viable cell numbers were then measured using the MTT assay. * $P < 0.05$, ** $P < 0.01$ and *** $P < 0.001$ vs. Aur at the indicated concentrations. (D and E) BT-549 cells were cultured in the absence (open circles) or presence of $0.31 \mu\text{M}$ MI-463 (open triangles), $0.2 \mu\text{M}$ Aur (open squares), or MI-463 ($0.31 \mu\text{M}$) plus Aur ($0.2 \mu\text{M}$) (closed circles) for the indicated number of days. The (D) viable cell number and (E) viability were assessed by the trypan blue dye exclusion assay using the automated cell counter model R1. (F) BT-549 cells were cultured in the absence (open circles) or presence of $0.31 \mu\text{M}$ MI-463 (open triangles), $0.1 \mu\text{M}$ Aur (open squares), or MI-463 ($0.31 \mu\text{M}$) plus Aur ($0.1 \mu\text{M}$) (closed circles) for the indicated number of days. Viable cell numbers were measured using the trypan blue dye exclusion test. The culture medium was replaced by fresh medium once every 5 days. Cell density was maintained at $2\text{--}5 \times 10^4$ cell/ml. Data are representative of the means ± SD of 3 measurements. * $P < 0.05$, ** $P < 0.01$ and *** $P < 0.001$ vs. control at the indicated time points.

with MI-463 and auranofin on the proliferation of BT-549 cells (Fig. 3F) were also examined. The growth rate of MI-463 ($0.31 \mu\text{M}$)- or auranofin ($0.1 \mu\text{M}$)-treated cells was similar to that of the control cells until 20 days. On the other hand, cell growth was markedly inhibited by combined treatment with

MI-463 and auranofin at 5 and 10 days, and no live cells were detected after 15 days.

The effects of combined treatment with MI-463 and auranofin were further examined on various cancer cell lines. The IC₅₀ values of MI-463 alone in the human mammary cancer

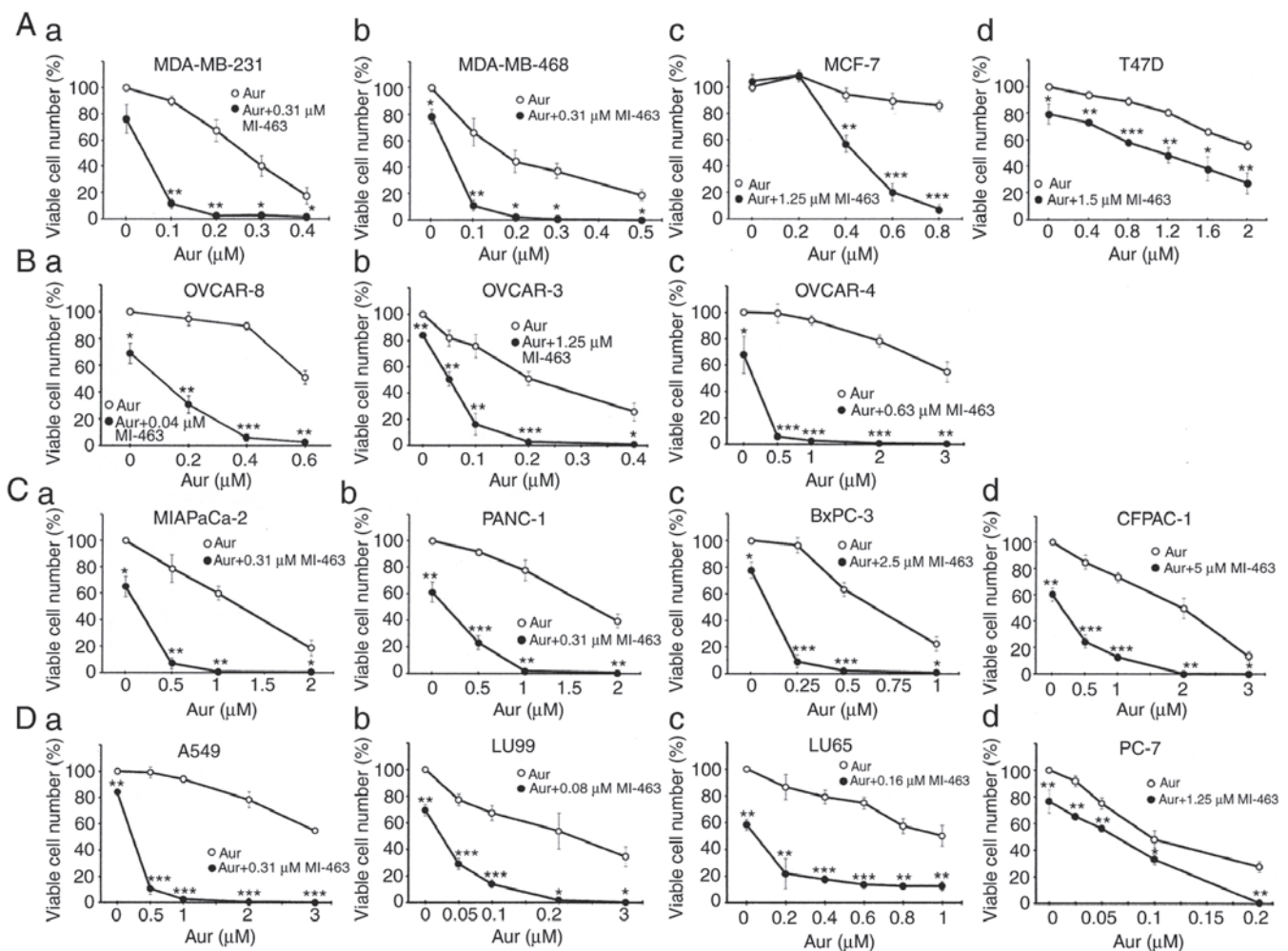


Figure 4. (A) Effects of combined treatment with MI-463 and auranofin (Aur) on the viability of breast carcinoma cells. (A-a) MDA-MB-231, (A-b) MDA-MB-468, (A-c) MCF-7, and (A-d) T47D cells were cultured with Aur in the absence (open circles) or presence of (A-a and A-b) 0.31 μ M, (A-c) 1.25 μ M, or (A-d) 1.5 μ M MI-463 (closed circles) for 4 days. (B) Effects of combined treatment with MI-463 and Aur on the viability of ovarian carcinoma cells. (B-a) OVCAR-8, (B-b) OVCAR-3 and (B-c) OVCAR-4 cells were cultured with Aur in the absence (open circles) or presence of 0.04 μ M (A-a), 1.25 μ M (B-b), and 0.63 μ M (B-c) MI-463 (closed circles) for 4 days. (C) Effects of combined treatment with MI-463 and Aur on the viability of pancreatic cancer cells. (C-a) MIAPaCa-2, (C-b) PANC-1, (C-c) BxPC-3, and (C-d) CFPAC-1 cells were cultured with Aur in the absence (open circles) or presence of (C-a and C-b) 0.31 μ M, (C-c) 2.5 μ M, or (C-d) 5 μ M MI-463 (closed circles) for 4 days. (D) Effects of combined treatment with MI-463 and Aur on the viability of lung carcinoma cells. (D-a) A549, (D-b) LU99, (D-c) LU65, and (D-d) PC-7 cells were cultured with Aur in the absence (open circles) or presence of (D-a) 0.31 μ M, (D-b) 0.08 μ M, (D-c) 0.16 μ M, or (D-d) 1.25 μ M MI-463 (closed circles) for 4 days. Viable cell numbers were then measured using the MTT assay. Data are representative of the means \pm SD of 3 measurements. * P <0.05, ** P <0.01 and *** P <0.001 vs. Aur at the indicated concentrations.

cell lines, MDA-MB-231, MDA-MB-468, MCF-7 and T47D, were 0.48, 0.63, 5.0 and 2.5 μ M, respectively (data not shown). The effects of combined treatment with MI-463 and auranofin were also examined on another 4 human mammary cancer cell lines (Fig. 4A). MI-463 (0.31 μ M) significantly enhanced the auranofin-induced suppression of the viable cell number of the triple-negative breast cancer cell lines, MDA-MB-231 and MDA-MB-468 (Fig. 4A-a and b), as well as that of the BT-549 cells (Fig. 3B). However, MI-463 alone, even at the concentration of 1.25 μ M, did not affect the viable number of MCF-7 cells (data not shown), and auranofin alone, even at a high concentration (0.8 μ M), only slightly reduced the viable cell number to ~90% of the control, whereas auranofin at 0.4, 0.6 or 0.8 μ M significantly reduced the viable number of MCF-7 cells to ~50, 20 or <10% of the control, respectively, in the presence of 1.25 μ M MI-463 (Fig. 4A-c). On the other hand, treatment with MI-463 (1.5 μ M) alone reduced the

viable cell number to 80% of the control in the T47D cells (data not shown) and combined treatment with MI-463 and auranofin only exerted additive effects on growth suppression (Fig. 4A-d).

The IC_{50} values of MI-463 alone in the human ovarian cancer cell lines, OVCAR-8 (Fig. 1A), OVCAR-3 and OVCAR-4 were 0.06, >1.25 (data not shown) and >1.25 μ M (data not shown), respectively. The effects of combined treatment with MI-463 and auranofin on 3 human ovarian cancer cell lines were then examined (Fig. 4B). MI-463 and auranofin synergistically reduced the viable number of OVCAR-8, OVCAR-3 and OVCAR-4 cells (Fig. 4B-a, b and c). Although treatment with MI-463 (0.04 μ M) alone reduced the viable cell number to ~70% of the control in OVCAR-8 cells (Fig. 1A), and auranofin (0.4 μ M) alone reduced the viable cell number to ~90% of the control in OVCAR-8 cells, combined treatment with MI-463 (0.04 μ M) and auranofin (0.4 μ M) reduced the

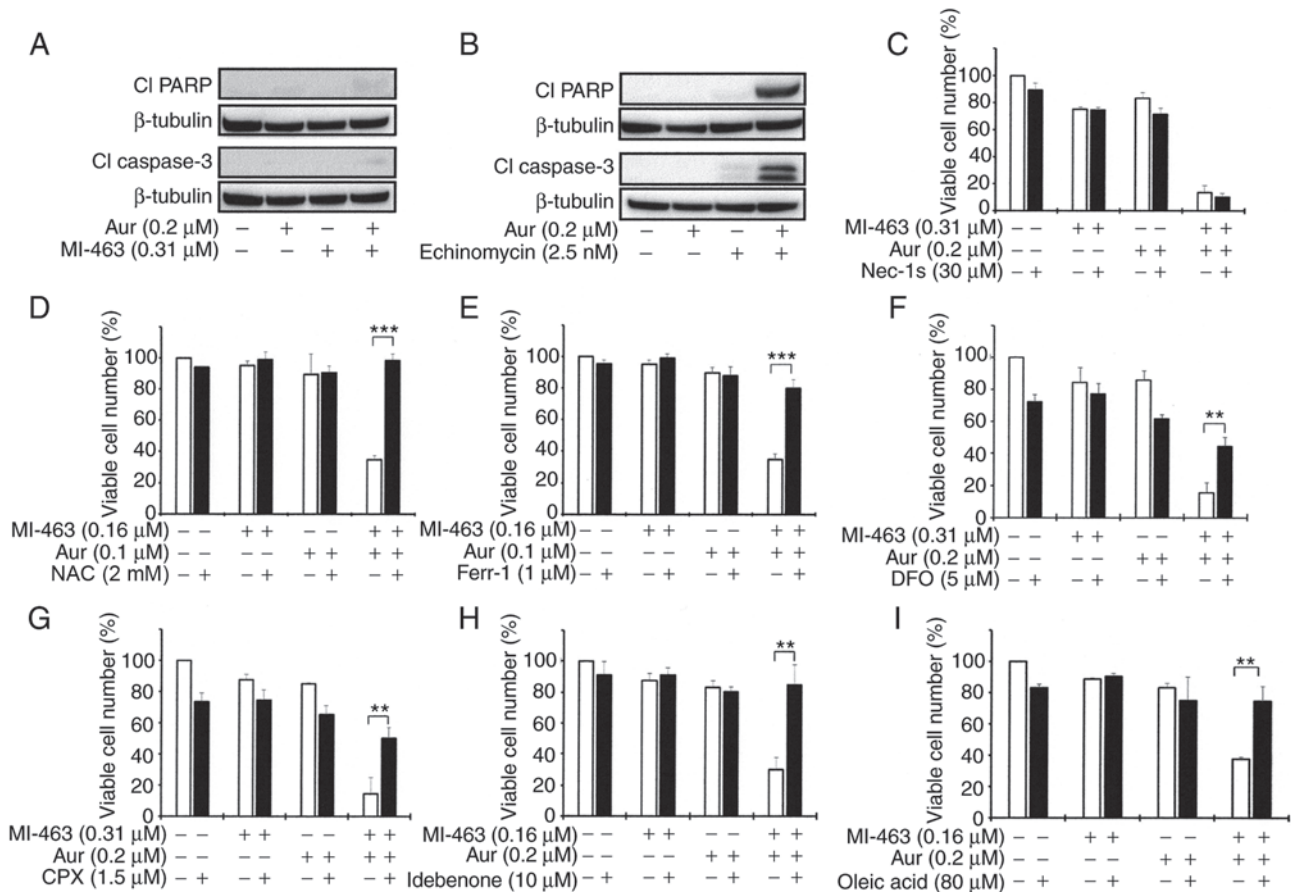


Figure 5. Effects of several ferroptosis inhibitors on the MI-463 plus auranofin (Aur)-induced cell death of BT-549 cells. (A and B) Western blot analyses of cleaved PARP (Cl. PARP), cleaved caspase-3 (Cl. Caspase-3) and β -tubulin. (A) BT-549 cells were cultured with or without 0.31 μ M MI-463, 0.2 μ M Aur, or MI-463 (0.31 μ M) plus Aur (0.2 μ M) for 24 h. (B) BT-549 cells were cultured with or without 2.5 nM echinomycin, 0.2 μ M Aur, or echinomycin (2.5 nM) plus Aur (0.2 μ M) for 24 h. Whole cell lysates were used for western blot analysis. The protein expression of β -tubulin served as the loading control. Similar results were obtained in 2 additional experiments. (C-I) BT-549 cells were treated with (D, E, H and I) 0.16 μ M or (C, F and G) 0.31 μ M MI-463, (D and E) 0.1 μ M or (C and F-I) 0.2 μ M Aur, or (C) MI-463 plus Aur in the presence or absence of 30 μ M Nec-1s, (D) 2 mM N-acetylcysteine (NAC), (E) 1 μ M ferrostatin-1 (Ferr-1), (F) 5 μ M deferoxamine (DFO), (G) 1.5 μ M ciclopirox (CPX), (H) 10 μ M idebenone, or (I) 80 μ M oleic acid for 3 days. Cells were treated with Nec-1s, NAC, Ferr-1, DFO, CPX, idebenone, or oleic acid for 2 h prior to the MI-463, Aur, or MI-463 plus Aur treatment. Viable cell numbers were measured by MTT assay. Data are representative of the means \pm SD of 3 measurements. ** P <0.01 and *** P <0.001.

viable cell number to <10% of the control in OVCAR-8 cells (Fig. 4B-a).

The IC_{50} values of MI-463 alone in the human pancreatic cancer cell lines, MIAPaCa-2, PANC-1, BxPC-3 and CFPAC-1, were 0.63, 0.60, 3.7 and 6.5 μ M, respectively (data not shown). The effects of combined treatment with MI-463 and auranofin on 4 human pancreatic cancer cell lines were then examined (Fig. 4C). MI-463 and auranofin synergistically reduced the viable number of MIAPaCa-2, PANC-1, BxPC-3 and CFPAC-1 cells (Fig. 4C).

The IC_{50} values of MI-463 alone in the human lung cancer cell lines, A549, LU99, LU65 and PC-7 cells, were >1.25, 0.50, 0.24 and 2.4 μ M, respectively (data not shown). The effects of combined treatment with MI-463 and auranofin on 4 human lung cancer cell lines were then examined (Fig. 4D). MI-463 and auranofin synergistically reduced the viable number of A549, LU99 and LU65 cells (Fig. 4D-a, b and c). On the other hand, MI-463 (1.25 μ M) alone reduced the viable cell number to ~80% of the control in PC-7 cells (data not shown), whereas combined treatment with MI-463 and auranofin only exerted additive effects on growth suppression (Fig. 4D-d). Collectively, these results indicated that synergistic growth

suppressive effects were induced by combined treatment with MI-463 and auranofin in 88% (14/16 cell lines) of the cancer cell lines tested: All 3 ovarian cancer cell lines, 4 out of 5 breast cancer cell lines, all of pancreatic cancer cell lines, and 3 out of 4 lung cancer cell lines.

MI-463 and auranofin synergistically induce ferroptotic cancer cell death. The present study then investigated whether the synergistic induction of cancer cell death by combined treatment with MI-463 and auranofin was due to ferroptosis. MI-463 (0.31 μ M) alone, auranofin (0.2 μ M) alone, or combined treatment with MI-463 (0.31 μ M) and auranofin (0.2 μ M) did not induce the expression of typical apoptotic markers, such as cleaved PARP and cleaved caspase-3 in the BT-549 cells (Fig. 5A). Since it was demonstrated that combined treatment with echinomycin (2.5 nM) and auranofin (0.2 μ M) induced apoptosis (unpublished data, in preparation), the present used echinomycin (2.5 nM) plus auranofin (0.2 μ M) as a positive control for cleaved PARP and cleaved caspase-3 (Fig. 5B). In addition, the necroptosis inhibitor, Nec-1s, failed to suppress the cell death induced by MI-463 plus auranofin (Fig. 5C). Treatment with MI-463 (0.16 μ M) and auranofin (0.1 μ M) for

3 days markedly decreased the viable cell number to ~30%, while treatment with MI-463 alone or auranofin alone did not significantly reduce the viable cell number (Fig. 5D). Treatment with the ROS scavenger, NAC (2 mM), almost completely abrogated the decrease in the viable cell number induced by MI-463 plus auranofin (Fig. 5D). Treatment with the ferroptosis inhibitor, Ferr-1 (1 μ M), evidently abolished the MI-463 plus auranofin-induced decrease in the viable cell number (Fig. 5E). The iron chelators, DFO (5 μ M) (Fig. 5F) and CPX (1.5 μ M) (Fig. 5G), also markedly abolished the MI-463 plus auranofin-induced decrease in the viable cell number. It was also found that DFO significantly attenuated ferroptotic cell death induced by MI-463 plus auranofin in p53 wild-type MCF-7 cells (data not shown). These results suggest that the attenuation of ferroptotic cell death by iron chelators is not affected by the status of the p53 gene. Furthermore, co-treatment with idebenone (a membrane-permeable analog of CoQ10) (Fig. 5H) or oleic acid (a monounsaturated fatty acid) (Fig. 5I) blocked the MI-463 plus auranofin-induced decrease in the viable cell number. On the other hand, the induction of cell death by auranofin alone at higher concentrations (2-4 μ M) was also abolished by NAC, but not by Ferr-1 and DFO (data not shown). Similar results were obtained in OVCAR-8 cells (data not shown). These results suggested that the synergistic cell death induced by combined treatment with MI-463 and auranofin was mainly due to the induction of ferroptosis.

Inhibitors of SCD1 synergistically induce cancer cell death in combination with auranofin, but not with MI-463. Since oleic acid (a monounsaturated fatty acid and one of the end products of SCD1) blocked the MI-463 plus auranofin-induced decrease in viable cell numbers (Fig. 5I), the present study then investigated whether inhibitors of SCD1, similar to MI463, can enhance cancer cell death synergistically with auranofin. CAY10566 and MF-438, two chemically distinct pharmacological inhibitors of SCD1 enzymatic activity, were used. Auranofin alone, even at the concentration of 0.2 μ M, decreased the viability of BT-549 cells to ~70% of the control (Fig. 6A and B), and CAY10566 (10 μ M) or MF-438 (3 μ M) alone decreased the viability of BT-549 cells to ~80% of the control, whereas auranofin at 0.1 or 0.2 μ M reduced the viability of BT-549 cells to ~25 or 10% of the control, respectively, in the presence of CAY10566 (10 μ M) (Fig. 6A) or MF-438 (3 μ M) (Fig. 6B). The synergistic induction of cell death in combination with auranofin and SCD1 inhibitors was evidently abrogated by Ferr-1 (data not shown). These results indicated that inhibitors of SCD1, similar to MI-463, induced ferroptotic cancer cell death synergistically with auranofin. On the other hand, CAY10566 (10 μ M) could not enhance the MI-463-induced death of BT-549 cells, but rather CAY10566 at 10 μ M interfered with the cell death-inducing activity of MI-463 at 0.31 or 0.63 μ M (Fig. 6C). MF-438 at 3 μ M also interfered with the cell death-inducing activity of MI-463 at 0.63 μ M (data not shown). These results suggest that the MI-463-induced decrease in cell viability may be due at least in part to the inhibition of SCD1 activity.

MI-463 enhances auranofin-induced HO-1 expression. Previous studies (24-27) have demonstrated that HO-1

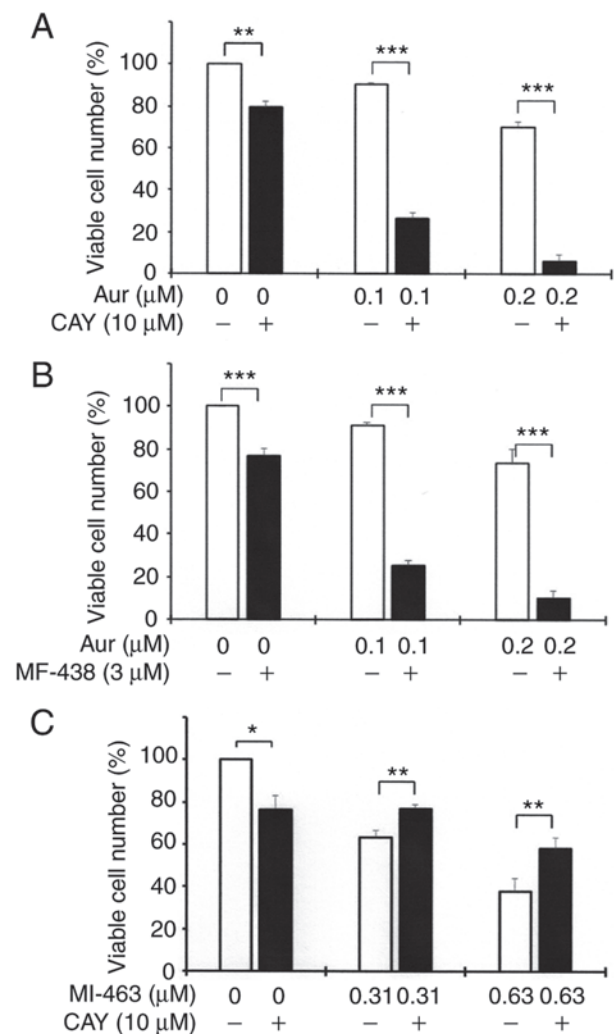


Figure 6. Effects of inhibitors of stearoyl-CoA desaturase 1 (SCD1) on the auranofin (Aur)- or MI-463-induced cell death of BT-549 cells. BT-549 cells were treated with 0.1 or 0.2 μ M Aur in the presence or absence of 10 μ M CAY10566 (CAY) (A) or 3 μ M MF-438 (B) for 3 days. (C) BT-549 cells were treated with 0.31 μ M or 0.63 μ M MI-463 in the presence or absence of 10 μ M CAY for 3 days. Cells were treated with CAY or MF-438 for 2 h prior to the Aur or MI-463 treatment. Viable cell numbers were measured by MTT assay. Data are representative of the means \pm SD of 3 measurements. * P <0.05, ** P <0.01 and *** P <0.001.

accelerates erastin-induced ferroptotic cell death and that HO-1 is a major intracellular source of iron. Therefore, the present study examined whether ferroptotic cell death induced by MI-463 and auranofin was accompanied by the induction of HO-1 expression. The expression of HO-1 was approximately 17- or 18-fold higher in the auranofin (0.2 μ M)-treated BT-549 cells than in the control cells at 12 or 24 h, respectively (Fig. 7A), whereas the MI-463 (0.16 μ M)-treated cells did not exhibit a significant increase (Fig. 7A). Furthermore HO-1 gene expression was markedly induced (~60 or 70-fold) in the MI-463 (0.16 μ M) plus auranofin (0.2 μ M)-treated BT-549 cells at 12 or 24 h, respectively (Fig. 7A). Similar results were obtained when the OVCAR-8, MDA-MB-231, PANC-1 or A549 cells were treated with MI-463 plus auranofin for 24 h (data not shown). HO-1 protein expression was also markedly increased (~16-fold) in the MI-463 (0.16 μ M) plus auranofin (0.2 μ M)-treated BT-549 cells at 24 h, whereas the protein level

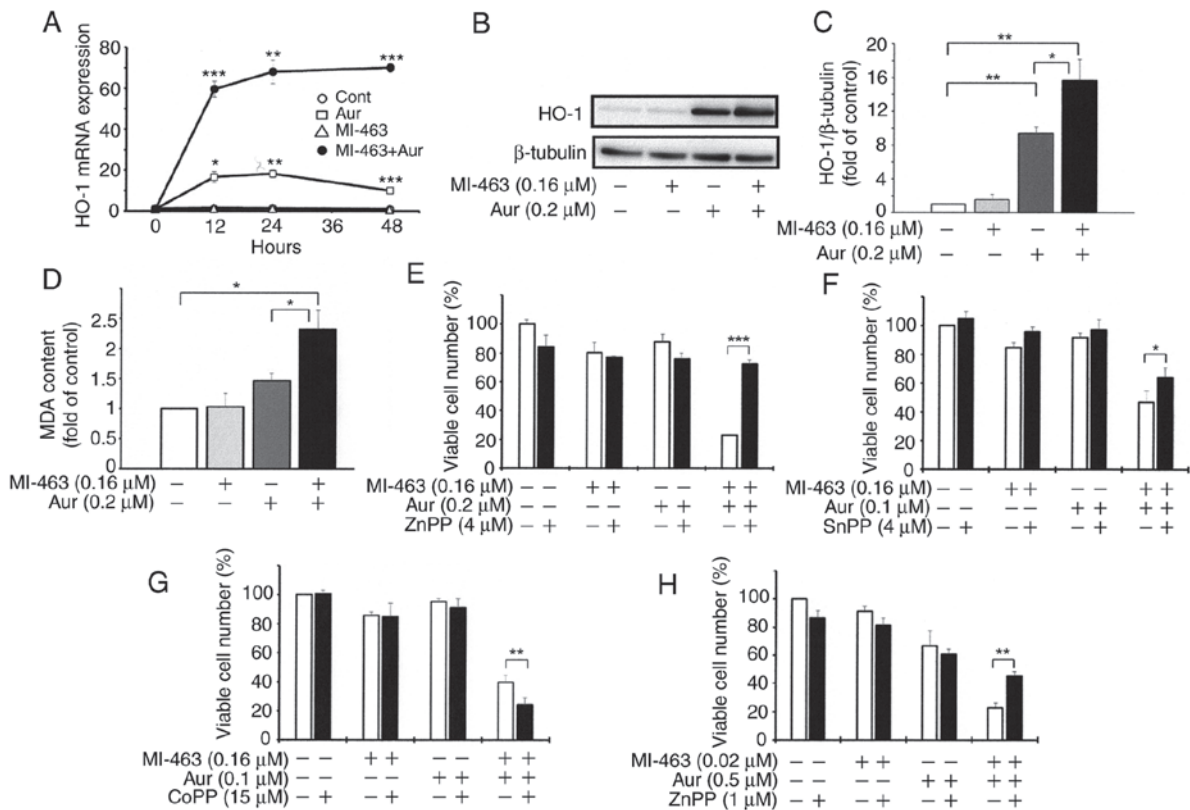


Figure 7. Effects of heme oxygenase-1 (HO-1) on the MI-463 plus auranofin (Aur)-induced death of BT-549 or OVCAR-8 cells. (A) MI-463 markedly enhanced Aur-induced HO-1 gene expression in BT-549. BT-549 cells (1.5×10^4 cells/ml) were cultured without (open circle) or with $0.16 \mu\text{M}$ MI-463 (open triangle), $0.2 \mu\text{M}$ Aur (open square), or $0.16 \mu\text{M}$ MI-463 plus $0.2 \mu\text{M}$ Aur (closed circle) for the indicated periods of time. HO-1 gene expression was examined by RT-qPCR. Data are representative of the means \pm SD of 3 measurements. * $P < 0.05$, ** $P < 0.01$ and *** $P < 0.001$ vs. control at the indicated time points. (B and C) Western blot analysis of HO-1 and β -tubulin. BT-549 cells were cultured with or without $0.16 \mu\text{M}$ MI-463, $0.2 \mu\text{M}$ Aur, or MI-463 ($0.16 \mu\text{M}$) plus Aur ($0.2 \mu\text{M}$) for 24 h. Whole cell lysates were used for western blot analysis. The protein expression of β -tubulin served as the loading control (representative blots are shown in panel B). (C) Quantification of densitometric evaluation of the western blots; means \pm SD ($n=3$). (D) MI-463 markedly enhanced Aur-induced MDA accumulation in BT-549 cells. BT-549 cells (1.5×10^4 cells/ml) were cultured without or with $0.16 \mu\text{M}$ MI-463, $0.2 \mu\text{M}$ Aur, or $0.16 \mu\text{M}$ MI-463 plus $0.2 \mu\text{M}$ Aur for 24 h. (E-G) BT-549 cells were treated with (E-G) $0.16 \mu\text{M}$ MI-463, (F and G) $0.1 \mu\text{M}$ or (E) $0.2 \mu\text{M}$ Aur, or (E) MI-463 plus Aur in the presence or absence of $4 \mu\text{M}$ zinc protoporphyrin-IV (ZnPP), (F) $4 \mu\text{M}$ Tin protoporphyrin IV (SnPP), or (G) $15 \mu\text{M}$ cobalt protoporphyrin IV CoPP for 3 days. Cells were treated with ZnPP, SnPP, or CoPP for 2 h prior to the MI-463, Aur, or MI-463 plus Aur treatment. Viable cell numbers were measured by MTT assay. (H) OVCAR-8 cells were treated with $0.02 \mu\text{M}$ MI-463, $0.5 \mu\text{M}$ Aur, or MI-463 plus Aur in the presence or absence of $1 \mu\text{M}$ ZnPP for 3 days. Cells were treated with ZnPP for 2 h prior to the MI-463, Aur, or MI-463 plus Aur treatment. Viable cell numbers were measured by MTT assay. Data are representative of the means \pm SD of 3 measurements. * $P < 0.05$, ** $P < 0.01$ and *** $P < 0.001$.

of HO-1 was approximately 9-fold higher in the BT-549 cells treated with auranofin alone than in the control cells at 24 h (Fig. 7B and C). The BT-549 cells treated with MI-463 alone only exhibited a slight increase in HO-1 protein levels (Fig. 7B and C). MDA is one of the end products of lipid peroxidation and one of the typical evaluation markers of the degree of cell ferroptosis (13).

The present study then examined whether MDA was induced during MI-463 plus auranofin-induced ferroptosis. The MDA content was significantly increased in the MI-463 plus auranofin-treated BT-549 cells at 24 h (Fig. 7D). Subsequently, whether inhibitors of HO-1 attenuate the ferroptotic death of BT-549 cells induced by MI-463 plus auranofin was examined. Treatment with ZnPP, a specific inhibitor of HO-1, markedly attenuated the MI-463 plus auranofin-induced death of BT-549 cells (Fig. 7E). Similar results were obtained in the breast cancer cell line, MDA-MB-231 (data not shown). Treatment with SnPP, another specific inhibitor of HO-1, also significantly attenuated the MI-463 plus auranofin-induced death of BT-549 cells (Fig. 7F). Treatment with CoPP, an inducer of

HO-1, stimulated the MI-463 plus auranofin-induced death of BT-549 cells (Fig. 7G). It was also found that ZnPP attenuated ferroptotic cancer cell death induced by MI-463 plus auranofin in the ovarian cancer cell line, OVCAR-8 (Fig. 7H). These results suggest that the induction of HO-1 is associated at least in part with the induction of ferroptotic cancer cell death by combined treatment with MI-463 plus auranofin.

Discussion

The inhibition of the menin-MLL interaction has recently emerged as a novel therapeutic strategy. Menin-MLL inhibitors, such as MI-463, MI-503, MI-3454 and VTP50469, markedly inhibit the proliferation and induce the differentiation of acute leukemia cells and primary patient samples with MLL translocations or NPM1 mutations (1,3-5). Furthermore, these inhibitors have been attracting attention as a therapeutic method for not only leukemia, but also solid cancers (2,6-9). Zhu *et al* previously reported that p53 GOF mutants bound to and upregulated chromatin regulatory genes, such as MLL1,

resulting in genome-wide increases in histone methylation in some solid cancers, including breast cancer (2). The genetic knockdown of MLL reduced the proliferation of BT-549 (mutant p53 249S) and MDA-MB-468 (mutant p53 R273H) cells, but exerted a negligible effect on the proliferation of MCF-7 (wild-type p53) cells (2). Dreijerink *et al* (6) reported that the genetic knockdown of menin reduced the estradiol- or epidermal growth factor-induced proliferation of MCF-7 cultured in phenol red-free medium containing 10% charcoal dextran-treated fetal bovine serum, but did not describe the effects of the genetic knockdown of menin on the proliferation of ER-negative breast cancer cells. In the present study, it was found that the proliferation of the triple-negative breast cancer cells, BT-549 (IC₅₀ value, 0.40 μ M) and MDA-MB-468 cells (IC₅₀ value, 0.63 μ M) (data not shown), was efficiently reduced by the menin-MLL inhibitor MI-463 at a lower concentration than that of the MCF-7 cells (IC₅₀ value, 5.0 μ M) (data not shown). These results are consistent with the genetic knockdown findings previously reported by Zhu *et al* (2), but not by Dreijerink *et al* (6). The proliferation of the MCF-7 cells specifically induced by estradiol- or epidermal growth factor may also be dependent on menin-MLL. The MDA-MB-231 (p53 mutant R280K) cells were also sensitive to MI-463 (IC₅₀ value, 0.48 μ M) (data not shown). Although the T47D cells have the p53 mutant L194F, which is also GOF p53, the T47D cells were less sensitive to MI-463 (IC₅₀ value, 2.5 μ M) (data not shown) than the other breast cancer cells with mutant p53. Since the genetic knockdown of MLL also reduced the proliferation of pancreatic cancer PANC-1 cells (p53 mutant R273H), as well as p53 mutant breast cancer cells (2), the present study examined the effects of MI-463 on the proliferation of several types of cancer cell lines (16 cell lines, including human breast cancer and pancreatic cancer cell lines). All 4 cell lines with wild-type (MCF-7, A549 and PC-7) and null (OVCAR-3) type p53 exhibited IC₅₀ values >1 μ M. However, p53 gene mutation was apparently not a sole factor which affected the sensitivity to MI-463, as PC-7 (wild-type p53) and OVCAR-3 (null-type p53) exhibited similar sensitivities to MI-463 (Fig. 4B-b and D-d). On the other hand, the IC₅₀ values for 8/12 (68%) cell lines with the p53 mutant and 6/7 (86%) cell lines with the p53 mutant plus KRAS mutant were <1 μ M. These results suggest that sensitivity to menin-MLL inhibitors, such as MI-463, is dependent not only on the p53 status, but also on the KRAS mutation in several solid cancer cells.

The OVCAR-8 human ovarian cancer cells exhibited the greatest susceptibility to MI-463-induced growth inhibitory effects (IC₅₀ value, 0.06 μ M) in the present study (Fig. 1A). The growth inhibitory effects induced by MI-503 (IC₅₀ value, 0.04 μ M) were similar to those induced by MI-463 (Fig. 1A and B). Borkin *et al* (3) reported that MI-463 and MI-503 similarly demonstrated their pronounced effects in blocking MLL leukemia progression *in vivo* and that MI-463 and MI-503 are two lead compounds with comparable efficacy and druglike properties. MI-463 was used mainly in the present study, since MI-463 markedly induced ferroptosis almost comparable to that induced by MI-503, and MI-463 was much less costly than MI-503. The growth inhibitory effects induced by MI-2-2 (IC₅₀ value, 1.4 μ M) were markedly weaker than those induced by MI463 and MI-503 (Fig. 1A). Borkin *et al* (3) previously reported that the treatment of

murine bone marrow cells, which had been transformed with the MLL-AF9 oncogene, with MI-463 and MI-503 markedly inhibited growth, with IC₅₀ values of 0.23 and 0.22 μ M, respectively, measured after 7 days of treatment; the growth inhibitory effects induced by MI-2-2 (IC₅₀ value, 1.3 μ M) were also markedly weaker than those induced by MI463 and MI-503. The potency of the growth inhibitory activities of MI-463, MI-503 and MI-2-2 in MLL-leukemia cells was associated with the potency of the inhibitory activities of the menin-MLL interaction by MI-463, MI-503 and MI-2-2: The IC₅₀ values were 15.3, 14.7 and 46 nM, respectively (3,28). Therefore, the selective killing of OVCAR-8 cells by MI-463, MI-503 and MI-2-2 may also be attributed to the inhibition of the menin-MLL interaction, although a recent study (29) reported that the menin-MLL complex was not essential for the survival of most solid cancer models. In this regard, the present study examined whether VTP50469, another recently reported potent menin-MLL inhibitor (30,31), could induce the ferroptotic death of OVCAR-8 ovarian cancer cells. The preliminary results revealed that VTP50469 did not induce the death of OVCAR-8 cells even at a high concentration (10 μ M) (Fig. 1D). These results suggest the possibility that MI-463, MI-503 and MI-2-2 may induce cell death independent of menin-MLL inhibition. Further research is required to reach definitive conclusions.

The inhibition of the menin-MLL interaction with small-molecule inhibitors, such as MI-463, MI-503, MI-3454 and VTP50469, was previously shown to inhibit cell proliferation and induce the differentiation and mild apoptosis in MLL1-rearranged and NPM1-mutated leukemia. The beneficial therapeutic effects of these inhibitors have also been proposed in several solid tumors (3-5). However, the mechanisms of induction of cell death induced by inhibitors of the menin-MLL interaction have not yet been elucidated in detail. The present study demonstrated for the first time, at least to the best of our knowledge, that menin-MLL inhibitors, such as MI-463, induce cell death by inducing ferroptosis in some types of cancer cells. As described above, MI-463 markedly reduced the viable number of OVCAR-8 cells at 3 days (Fig. 1). MI-463 significantly induced ROS production at 8 h and further increased ROS generation at 24 h (Fig. 2B). NAC (a ROS scavenger) efficiently reversed MI-463-induced cell death (Fig. 2A). MI-463-induced cell death was also inhibited by ferroptosis inhibitors (Ferr-1, PD146176 and idebenone) and iron chelators (DFO and CPX), but not by the apoptosis inhibitor, Z-VAD (Fig. 2). These results suggest that MI-463 induces cancer cell death through the induction of ferroptosis in some types of cancer cells.

Auranofin was approved by the US Food and Drug Administration (FDA) for the treatment of rheumatoid arthritis in 1985 (32) (Drugs@FDA:FDA-Approved Drugs (<https://www.accessdata.fda.gov>)). It was recently investigated as a potential therapeutic agent for human cancers, including ovarian, breast, pancreatic and lung cancers (33-36). TrxR is an enzyme in the thioredoxin system that is important for maintaining the intracellular redox state. TrxR overexpression has been shown to be associated with an aggressive tumor progression and the poor survival of patients with breast, ovarian and lung cancers (32). Auranofin inhibits the activity of TrxR, increases cellular oxidative stress, particularly in cancer and induces

apoptosis (32-36). The present study found that combined treatment with auranofin at concentrations that did not induce apoptosis and MI463 at concentrations that only weakly induced ferroptosis markedly enhanced the ferroptotic death of several cancer cell lines. This synergistic induction of cancer cell death by combined treatment was frequently observed: A total of 14 out of the 16 cancer cell lines tested (88%). The results of the present study also suggest that the synergistic effects of MI-463 and auranofin were unrelated to the inhibitory effects of MLL/WDR5 (a subunit of the MLL/COMPASS complex) protein-protein interaction inhibitors, because the combined treatment with auranofin and OICR-9429 (an antagonist of the interaction of MLL with WDR5) exerted only additive effects on the suppression of viable cancer cells (Fig. 3C). Another MLL/WDR5 protein-protein interaction inhibitor (Piribedil) and auranofin also did not induce synergistic cell death of BT-459 cells (data not shown). Both OICR-9429 and Piribedil have been reported to induce menin-MLL inhibition, growth suppression and differentiation of MLL-rearranged leukemia cells (23,37). Therefore, alternatively, the synergistic effect of MI-463 and auranofin may be independent of menin-MLL inhibition. The molecular mechanisms underlying the synergistic interaction between MI-463 and auranofin need to be elucidated in more detail in the future. Nevertheless, the high-frequency synergistic induction of cancer cell death with MI-463 plus auranofin strongly suggests that it may be useful for the future development of chemotherapy. Accumulating evidence suggests the potential of ferroptosis induction therapy as a novel cancer treatment strategy, particularly for eradicating aggressive malignancies that are resistant to traditional therapies (10,11,38). Paclitaxel-resistant BT-549 cells (BT-549/PacR) were obtained following a long-term culture in the presence of paclitaxel (final concentration at 100 nM). The proliferation of parental BT-549 cells was dose-dependently inhibited by paclitaxel (IC₅₀ value, 3.5 nM) (Table I), which is regarded as one of the first-line drugs in the treatment of breast cancer (39), whereas the proliferation of BT-549/PacR cells was not inhibited by paclitaxel, even at 100 nM (data not shown). MI-463 and auranofin also synergistically inhibited the proliferation of BT-549/PacR (data not shown). A similar synergistic growth inhibition by MI-463 plus auranofin was obtained when gemcitabine-resistant PANC-1 cells (PANC-1/GR) (20) were treated with MI-463 plus auranofin (data not shown). These results suggest that combined treatment with MI-463 plus auranofin has potential for use in the treatment of chemotherapy-resistant cancer.

SCD1 has previously been shown to be strongly expressed in ovarian cancer tissue and cell lines (16). Tesfay *et al* (16) recently reported that inhibitors of SCD1, such as CAY10566 and MF-438, induced lipid oxidation, decreased CoQ₁₀ and induced ferroptotic cell death, and also that oleic acid (a monounsaturated fatty acid and one of the end products of SCD1) protected against ferroptotic cell death induced by inhibitors of SCD1 in ovarian cancer cells. Furthermore, it was demonstrated that MI-463-induced cell death was inhibited by oleic acid in the ovarian cancer cell line, OVCAR-8 (Fig. 2H). These results indicate that the induction of ferroptotic cancer cell death induced by MI-463 is mediated by the modulation of SCD1; however, recent findings indicate that co-treatment with oleic acid also blocked ferroptosis induced

by other typical ferroptosis inducers (16,40). The results of the present study revealed that inhibitors of SCD1 (CAY10566 and MF-438), similar to MI463, enhanced cancer cell death synergistically with auranofin (Fig. 6A and B). On the other hand, CAY10566 did not additively induce cell death, but rather CAY10566 at 10 μ M interfered with the cell death-inducing activity of MI-463 at 0.31 or 0.63 μ M (Fig. 6C). MF-438 at 3 μ M also interfered with the cell death-inducing activity of MI-463 at 0.63 μ M (data not shown). If the specific activity of inhibition for the SCD1 enzyme is lower in CAY10566 than in MI-463, it may be possible to explain these results. Although further experiments are required, it is possible that the MI-463-induced decrease in cell viability may be due at least in part to the inhibition of SCD1 activity. Whether Menin-MLL inhibitors, such as MI-463, MI-503 and MI-2-2 can directly inhibit SCD1 activity will be an important issue to be solved in the future. A previous study reported that inhibitors of SCD1, such as CAY10566 and MF-438, enhanced ferroptotic cancer cell death induced by RSL3 (a typical ferroptosis inducer) in the ovarian cancer cell line OVCAR-4 (16). It was also found that menin-MLL inhibitors, such as MI-463 and MI-2-2, synergistically enhanced ferroptotic cancer cell death induced by RSL3 in the breast cancer cell line, BT-549, and the ovarian cancer cell line, OVCAR-8 (data not shown). The results of the present study suggest that menin-MLL inhibitors, such as MI-463 and MI-2-2, as well as SCD1 inhibitors, synergistically enhance RSL3-induced ferroptotic cancer cell death.

Normal cells with a lower basal ROS level are less dependent on antioxidants, rendering normal cells less sensitive to oxidative insults. Due to high proliferation and rapid metabolic rates, cancer cells produce more ROS, which may promote tumorigenesis and render cancer cells more vulnerable to oxidative stress-induced cell death. If increases in ROS reach a certain threshold level that is incompatible with cellular survival, ROS may exert cytotoxic effects, leading to the death of malignant cells and, thus, limiting cancer progression (2,27,41). HO-1 is commonly regarded as a survival molecule, playing an important role in cancer progression, and its inhibition is considered to be beneficial in a number of cancers. On the other hand, Gandini *et al* (42) reported that HO-1 plays an antitumor role in breast cancer. Furthermore, emerging evidence has indicated that HO-1 functions as a critical mediator in the induction of ferroptosis (24-26). Chiang *et al* (27) proposed a model for the HO-1-mediated induction of ferroptosis. HO-1 exerts cytoprotective effects by scavenging ROS during moderate activation. By contrast, the excessive activation of HO-1 increases labile Fe²⁺, leading to ROS overload and the death of cancer cells (27). It was observed that MI-463 markedly enhanced the auranofin-induced levels of both HO-1 mRNA and the HO-1 protein (Fig. 7A-C). The induction of ferroptotic cancer cell death by the combined treatment with MI-463 plus auranofin was attenuated by HO-1-specific inhibitors, such as ZnPP and SnPP, but was enhanced by a HO-1 inducer (CoPP) (Fig. 7E-G). Furthermore, combined treatment with MI-463 and auranofin only exerted additive effects on the growth suppression of T47D (Fig. 4A-d), and these additive growth inhibitory effects were not suppressed by HO-1-specific inhibitors (data not shown). These results suggest that the induction of HO-1 is involved, at least in part, in the induction

of ferroptotic cancer cell death by the combined treatment with MI-463 plus auranofin.

In conclusion, the present study demonstrated that menin-MLL inhibitors, such as MI-463, unexpectedly induced the ferroptotic death of several cancer cell line cells and that MI-463 in combination with auranofin, approved by the FDA for the treatment of rheumatoid arthritis, led to a synergistic increase in cancer cell death in breast, ovarian, pancreatic and lung cancer cell lines (88%, 14/16 cell lines). MI-463 achieved high levels in peripheral blood following a single intravenous or oral dose, while also exhibiting high oral bioavailability (~45%) in mice (3). Treatment with MI-463 (45 mg/kg, twice daily, p.o.) could maintain ~1 μ M MI-463 in plasma, and 20-day treatment of MLL-AF4 leukemia xenograft recipient mice with MI-463 resulted in a substantial delay in leukemia progression, whereas no decrease in body weight, organ weight, or tissue damage was observed upon treatment with MI-463 (3). Auranofin concentrations of 1-3 μ M in plasma are achievable without obvious side-effects in patient or volunteer subject who received the recommended dose of 6 mg/day for rheumatoid arthritis (43). These reports suggest that combination therapy of MI-463 and auranofin seems to be clinically applicable. Although the molecular mechanisms underlying the interaction between MI-463 and auranofin have not yet been elucidated in detail, the results presented herein suggest that menin-MLL inhibitors, such as MI-463, in combination with auranofin have potential for use as an effective therapeutic approach for several cancers via the induction of ferroptosis.

Acknowledgements

The authors would to acknowledge the technical expertise of the Interdisciplinary Center for Science Research Organization for Research and Academic Information, Shimane University.

Funding

The present study was partly supported by a grant from the Shimane University 'SUIGAN' project.

Availability of data and materials

The analyzed datasets generated during the study are available from the corresponding author on reasonable request.

Authors' contributions

All authors contributed to the manuscript as follows: IK, TK and SK were involved in the conceptualization of the study. IK and TK were involved in the study methodology. IK and TK were involved in the investigative aspects of the study and in the writing of the original draft. TK and SK were involved in the writing, revisions (reviewing) and editing of the manuscript, as well as in funding acquisition and study supervision. All authors have read and approved the final manuscript.

Ethics approval and consent to participate

Not applicable.

Patient consent for publication

Not applicable.

Competing interests

The authors declare that they have no competing interests.

References

1. Dawson MA and Kouzarides T: Cancer epigenetics: From mechanism to therapy. *Cell* 150: 12-27, 2012.
2. Zhu J, Sammons MA, Donahue G, Dou Z, Vedadi M, Getlik M, Barsyte-Lovejoy D, Al-awar R, Katona W, Shilatifard A, *et al*: Gain-of-function p53 mutants co-opt chromatin pathways to drive cancer growth. *Nature* 525: 206-211, 2015.
3. Borkin D, He S, Miao H, Kempinska K, Pollock J, Chase J, Purohit T, Malik B, Zhao T, Wang J, *et al*: Pharmacologic inhibition of the Menin-MLL interaction blocks progression of MLL leukemia in vivo. *Cancer Cell* 26: 589-602, 2015.
4. Krivtsov AV, Evans K, Gadrey JY, Eschle BK, Hatton C, Uckelmann HJ, Ross KN, Perner F, Olsen SN, Pritchard T, *et al*: A menin-MLL inhibitor induces specific chromatin changes and eradicates disease in models of MLL-rearranged leukemia. *Cancer Cell* 36: 660-673.e11, 2019.
5. Klossowski S, Miao H, Kempinska K, Wu T, Purohit T, Kim E, Linhares BM, Chen D, Jih G, Perkey E, *et al*: Menin inhibitor MI-3454 induces remission in MLL1-rearranged and NPM1-mutated models of leukemia. *J Clin Invest* 130: 981-997, 2020.
6. Dreijerink KMA, Groner AC, Vos ESM, Font-Tello A, Gu L, Chi D, Reyes J, Cook J, Lim E, Lin CY, *et al*: Enhancer-mediated oncogenic function of the menin tumor suppressor in breast cancer. *Cell Rep* 18: 2359-2372, 2017.
7. Malik R, Khan AP, Asangani IA, Cieřlik M, Prensner JR, Wang X, Iyer MK, Jiang X, Borkin D, Escara-Wilke J, *et al*: Targeting the MLL complex in castration-resistant prostate cancer. *Nature Med* 21: 344-352, 2015.
8. Svoboda LK, Bailey N, Van Noord RA, Krook MA, Harris A, Cramer C, Jasman B, Patel RM, Thomas D, Borkin D, *et al*: Tumorigenicity of Ewing sarcoma is critically dependent on the trithorax proteins MLL1 and menin. *Oncotarget* 8: 458-471, 2017.
9. Kempinska K, Malik B, Borkin D, Klossowski S, Shukla S, Miao H, Wang J, Cierpicki T and Grembecka J: Pharmacologic inhibition of the menin-MLL interaction leads to transcriptional repression of PEG10 and blocks hepatocellular carcinoma. *Mol Cancer Ther* 17: 26-38, 2017.
10. Dixon SJ, Lemberg KM, Lamprecht MR, Skouta R, Zaitsev EM, Gleason CE, Patel DN, Bauer AJ, Cantley AM, Yang WS, *et al*: Ferroptosis: An iron-dependent form of nonapoptotic cell death. *Cell* 149: 1060-1072, 2012.
11. Viswanathan VS, Ryan MJ, Dhruv HD, Gill S, Eichhoff OM, Seashore-Ludlow B, Kaffenberger SD, Eaton JK, Shimada K, Aguirre AJ, *et al*: Dependency of a therapy-resistant state of cancer cells on a lipid peroxidase pathway. *Nature* 547: 453-457, 2017.
12. Hangauer MJ, Viswanathan VS, Ryan MJ, Bole D, Eaton JK, Matov A, Galeas J, Dhruv HD, Berens ME, Schreiber SL, *et al*: Drug-tolerant persister cancer cells are vulnerable to GPX4 inhibition. *Nature* 551: 247-250, 2017.
13. Stockwell BR, Friedmann Angeli JP, Bayir H, Bush AI, Conrad M, Dixon SJ, Fulda S, Gascón S, Hatzios SK, Kagan VE, *et al*: Ferroptosis: A regulated cell death nexus linking metabolism, redox biology, and disease. *Cell* 171: 273-285, 2017.
14. Bersuker K, Hendricks JM, Li Z, Magtanong L, Ford B, Tang PH, Roberts MA, Tong B, Maimone TJ, Zoncu R, *et al*: The CoQ oxidoreductase FSP1 acts parallel to GPX4 to inhibit ferroptosis. *Nature* 575: 688-692, 2019.
15. Doll S, Freitas FP, Shah R, Aldrovandi M, da Silva MC, Ingold I, Grocin AG, Xavier da Silva TN, Panzilius E, Scheel CH, *et al*: FSP1 is a glutathione-independent ferroptosis suppressor. *Nature* 575: 693-698, 2019.
16. Tesfay L, Paul BT, Konstorum A, Deng Z, Cox AO, Lee J, Furdui CM, Hegde P, Torti FM and Torti SV: Stearoyl-CoA desaturase 1 protects ovarian cancer cells from ferroptotic cell death. *Cancer Res* 79: 5355-5366, 2019.

17. Honma Y, Kasukabe T, Yamori T, Kato N and Sassa T: Antitumor effect of cotylenin A plus interferon-alpha: Possible therapeutic agents against ovary carcinoma. *Gynecol Oncol* 99: 680-688, 2005.
18. Honma Y, Ishii Y, Yamamoto-Yamaguchi Y, Sassa T and Asahi K: Cotylenin A, a differentiation-inducing agent, and IFN-alpha cooperatively induce apoptosis and have an antitumor effect on human non-small cell lung carcinoma cells in nude mice. *Cancer Res* 63: 3659-3666, 2003.
19. Kasukabe T, Okabe-Kado J, Kato N, Sassa T and Honma Y: Effects of combined treatment with rapamycin and cotylenin A, a novel differentiation-inducing agent, on human breast carcinoma MCF-7 cells and xenografts. *Br Cancer Res* 7: R1097-R1110, 2005.
20. Kasukabe T, Honma Y, Okabe-Kado J, Higuchi Y, Kato N and Kumakura S: Combined treatment with cotylenin A and phenethyl isothiocyanate induces strong antitumor activity mainly through the induction of ferroptotic cell death in human pancreatic cancer cells. *Oncol Rep* 36: 968-976, 2016.
21. Yamaguchi Y, Kasukabe T and Kumakura S: Piperlongumine rapidly induces the death of human pancreatic cancer cells mainly through the induction of ferroptosis. *Int J Oncol* 52: 1011-1022, 2018.
22. Maniwa Y, Kasukabe T and Kumakura S: Vitamin K2 and cotylenin A synergistically induce monocytic differentiation and growth arrest along with the suppression of c-MYC expression and induction of cyclin G2 expression in human leukemia HL-60 cells. *Int J Oncol* 47: 473-480, 2015.
23. Zhang X, Zheng X, Yang H, Yan J, Fu X, Wei R, Xu X, Zhang Z, Yu A, Zhou K, *et al*: Piribedil disrupts the MLL1-WDR5 interaction and sensitizes MLL-rearranged acute myeloid leukemia (AML) to doxorubicin-induced apoptosis. *Cancer Lett* 431: 150-160, 2018.
24. Hu B, Shi C, Xu C, Cao P, Tian Y, Zhang Y, Deng L, Chen H and Yuan W: Heme oxygenase-1 attenuates IL-1 β induced alteration of anabolic and catabolic activities in intervertebral disc degeneration. *Sci Rep* 6: 21190, 2016.
25. Kwon MY, Park E, Lee SJ and Chung SW: Heme oxygenase-1 accelerates erastin-induced ferroptotic cell death. *Oncotarget* 6: 24393-24404, 2015.
26. Chang LC, Chiang SK, Chen SE, Yu YL, Chou RH and Chang WC: Heme oxygenase-1 mediates BAY 11-7085 induced ferroptosis. *Cancer Lett* 416: 124-137, 2018.
27. Chiang SK, Chen SE and Chang LC: A dual role of heme oxygenase-1 in cancer cells. *Int J Mol Sci* 20: 39, 2019.
28. Shi A, Murai MJ, He S, Lund G, Hartley T, Purohit T, Reddy G, Chruszcz M, Grembecka J and Cierpicki T: Structural insights into inhibition of the bivalent menin-MLL interaction by small molecules in leukemia. *Blood* 120: 4461-4469, 2012.
29. Brzezinka K, Nevedomskaya E, Lesche R, Haegebarth A, Ter Laak A, Fernández-Montalván AE, Eberspaecher U, Werbeck ND, Moening U, Siegel S, *et al*: Characterization of the Menin-MLL interaction as therapeutic cancer target. *Cancers (Basel)* 12: 201, 2020.
30. Krivtsov AV, Evans K, Gadrey JY, Eschle BK, Hatton C, Uckelmann HJ, Ross KN, Perner F, Olsen SN, Pritchard T, *et al*: A Menin-MLL inhibitor induces specific chromatin changes and eradicates disease in models of MLL-rearranged leukemia. *Cancer Cell* 36: 660-673, 2019.
31. Uckelmann HJ, Kim SM, Wong EM, Hatton C, Giovinazzo H, Gadrey JY, Krivtsov AV, Rücker FG, Döhner K, McGeehan GM, *et al*: Therapeutic targeting of preleukemia cells in a mouse model of NPM1 mutant acute myeloid leukemia. *Science* 367: 586-590, 2020.
32. Onodera T, Momose I and Kawada M: Potential anticancer activity of auranofin. *Chem Pharm Bull (Tokyo)* 67: 186-191, 2019.
33. Park SH, Lee JH, Berek JS and Hu MC: Auranofin displays anticancer activity against ovarian cancer cells through FOXO3 activation independent of p53. *Int J Oncol* 45: 1691-1698, 2014.
34. Bajor M, Graczyk-Jarzynka A, Marhelava K, Kurkowiak M, Rahman A, Aura C, Russell N, Zych AO, Firczuk M, Winiarska M, *et al*: Triple combination of ascorbate, menadione and the inhibition of peroxiredoxin-1 produces synergistic cytotoxic effects in triple-negative breast cancer cells. *Antioxidants (Basel)* 9: 320, 2020.
35. Kshattrya S, Saha A, Gries P, Tiziani S, Stone E, Georgiou G and DiGiovanni J: Enzyme-mediated depletion of l-cyst(e)ine synergizes with thioredoxin reductase inhibition for suppression of pancreatic tumor growth. *NPJ Precis Oncol* 3: 16, 2019.
36. Li H, Hu J, Wu S, Wang L, Cao X, Zhang X, Dai B, Cao M, Shao R, Zhang R, *et al*: Auranofin-mediated inhibition of PI3K/AKT/mTOR axis and anticancer activity in non-small cell lung cancer cells. *Oncotarget* 7: 3548-3558, 2016.
37. Grebien F, Vedadi M, Getlik M, Giambruno R, Grover A, Avellino R, Skucha A, Vittori S, Kuznetsova E, Smil D, *et al*: Pharmacological targeting of the Wdr5-MLL interaction in C/EBP α N-terminal leukemia. *Nat Chem Biol* 11: 571-578, 2015.
38. Chen P, Li X, Zhang R, Liu S, Xiang Y, Zhang M, Chen X, Pan T, Yan L, Feng J, *et al*: Combinative treatment of β -elemene and cetuximab is sensitive to KRAS mutant colorectal cancer cells by inducing ferroptosis and inhibiting epithelial-mesenchymal transformation. *Theranostics* 10: 5107-5119, 2020.
39. Saloustros E, Mavroudis D and Georgoulas V: Paclitaxel and docetaxel in the treatment of breast cancer. *Expert Opin Pharmacother* 9: 2603-2616, 2008.
40. Badgley MA, Kremer DM, Maurer HC, DelGiorno KE, Lee HJ, Purohit V, Sagalovskiy IR, Ma A, Kapilian J, Firl CEM, *et al*: Cysteine depletion induces pancreatic tumor ferroptosis in mice. *Science* 368: 85-89, 2020.
41. Trachootham D, Alexandre J and Huang P: Targeting cancer cells by ROS-mediated mechanisms: A radical therapeutic approach? *Nat Rev Drug Discov* 8: 579-591, 2009.
42. Gandini NA, Alonso EN, Fermento ME, Mascaró M, Abba MC, Coló GP, Arévalo J, Ferronato MJ, Guevara JA, Núñez M, *et al*: Heme oxygenase-1 has an antitumor role in breast cancer. *Antioxid Redox Signal* 30: 2030-2049, 2019.
43. Han Y, Chen P, Zhang Y, Lu Y, Ding W, Luo Y, Wen S, Xu R, Liu P and Huang P: Synergy between auranofin and celecoxib against colon cancer in vitro and in vivo through a novel redox-mediated mechanism. *Cancers (Basel)* 11: 931, 2019.